Wide-Area Damping of Sub-synchronous Oscillations Excited by large Wind Power Plants

Cees van Vledder, Jose Rueda Torres, Alex Stefanov, Peter Palensky
Intelligent Electrical Power Grids
Delft University of Technology
Delft, The Netherlands
[c.a.vanvledder, j.l.ruedatorres, a.i.stevanov,p.palensky]@tudelft.nl

Olimpo Anaya-Lara
Department of Electric Power Engineering
NTNU Norwegian University of Science and Technology
Trondheim, Norway
olimpo.anaya-lara@ntnu.no

Bas Kruimer
Digital Grid Operations
DNV Energy Systems
Arnhem, The Netherlands
bas.kruimer@dnv.com

Francisco Gonzalez-Longatt
Dept. of Engineering
DIgEnSysLab
University of Exeter
Exeter, UK
fglongatt@fglongatt.org

***Abstract*—Power electronic interfaced generation (PEIG) has become significantly dominant in the electrical power grid. This development is leading to a decrease in systemic inertia and damping against electrical oscillations. This causes the introduction of new and faster dynamic phenomena. One of these phenomena is sub-synchronous control interaction (SSCI), occurring as sub-synchronous oscillations (SSOs) in the system. Several real-world events reported so far have been related with large wind power plants (WPPs) and the improper tuning of the grid side converter (GSC) of (type-4) fully rated converter (FRC) wind turbines. As other PEIG have similar topologies and control systems, it is a very relevant topic. Weak grid conditions often contribute to the risks of SSO events. This paper proposes supplementary wide-area damping (WAD) to the control system of the GSC, focused on damping excursions of the phase locked loop (PLL). Signals measured by a remote phasor measurement unit (PMU) are communicated to the control system, which uses it for dynamic damping control. The effects of the WAD are tested by comparing the results of linearization-based eigenvalue analysis with and without the addition of WAD. Supplementary analysis conducted by using time-domain simulations and Prony analysis confirm the positive effect of WAD. Numerical tests are performed in DIgSILENT PowerFactory 2023 SP2 on a modified IEEE-39 bus test system.**

***Index Terms*—Sub-synchronous oscillations, observability, phasor measurement units, control interaction, wide area monitoring and control**

I. Introduction

Power electronic interfaced generation (PEIG) have an increasingly prominent role in the generation mix in the electrical power system [1]. Wind power plants (WPP) have a large contribution in this regard. This leads to new and faster dynamic phenomena due to the reduction of synchronous generation and their corresponding inertia [2]. Because of the rapid transition in the electrical power system, the risk of unknown or not well understood phenomena increases. Sub-synchronous oscillations (SSOs) induced by large WPP are one of these phenomena which have caused challenges in the last couple of years [3] [4]. This is an oscillation in the power system with a frequency below the fundamental frequency but amplitudes which can exceed 1 p.u. in voltage or current.
Different categories of SSO are described in [5]. The first wind-related sub-synchronous events took place in 2009, where the combination of type-3, induction generators, and radially connected fixed series compensation (FSC) caused a sub-synchronous resonance [3]. In following years, similar events where reported in other parts of the USA and China [6] [7]. Solutions were put forward to prevent radial connection in combination with high levels of FSC [8].

In 2015, a new type of SSO was first observed in China without the presence of any FSC [9]. This event was later categorized by [5] as sub-synchronous control interaction (SSCI) and where followed in 2017 and 2019 by similar events in China [10] and the UK [4], respectively. The SSO in the UK led to the activation of the protection in the WPP, which in turn led to a significant loss of generation resulting in large load shedding.

Type-4 WPPs, using fully rated converters (FRC), are mainly involved in SSCI. This makes this topic also more relevant for different types of PEIG, such as photovoltaics, battery energy storage and high-voltage direct-current (HVDC) links that have very similar topologies and control systems for their converters. As these types of PEIG are the most important in the intended transition of the energy system, it is essential to understand SSCI and find ways to mitigate it.
Most SSCI has been caused by either improper tuning of the control parameters of the grid side converter (GSC) or weak grid conditions [4] [9] [10] [11]. A combination of the two is also possible.

Among relevant control parameters, the inner control loop and phase locked loop (PLL) have the most influence on the sub-synchronous behaviour of the WPP. Different methods are used to determine the influence of these control parameters. In [12], Fourier analysis of time-domain oscillations is used to determine the influence of different inner control loop parameters on the SSO frequency. In [13], a linearized state-space model is used to find the influence of control parameters of the inner control loop on the sub-synchronous damping and frequency.

The influence of the PLL is also investigated in literature. The PLL keeps track of the rotating frame of the fundamental

frequency at the bus the WPP is connected to. A deviation in the measured value can lead to wrong power and reactive output. In [9] a criteria is put forward on how the improper tuning of the PLL can lead to an amplification of a sub-synchronous disturbance. In the work of [14] and [15], the sensitivity of the sub-synchronous mode to the tuning of the PLL is investigated.

Hence, a lot of effort has been put into understanding the causes of SSCI and how tuning could be a solution. However, the ideal tuning is often only valid for a specific grid topology. When transmission lines are taken out of service, the grid can become weaker, subsequently leading to risks of a SSO. In [16], the need for supplementary damping system in the control systems of the GSC is addressed. This paper proposes an additional layer to the control system, focused on damping PLL signal oscillation by using remote measurements using phasor measurement unit (PMU) based measurements. The supplementary wide-area damping (WAD) preserves most of the original control system. This enables easier understanding and implementation of the WAD.

Section II of the paper describes the modified IEEE-39 bus system used to test WAD performance. Section III introduces the proposed modified control system for the WPP. It also describes the expected behaviour of the system. In section IV the implemented WAD is tested and compared to the original control system of the WPP. First, eigenvalue analysis is performed, which compares the sub-synchronous modes and the corresponding participation factors. This is followed by time-domain simulations where the system response is tested in response to disturbances. These results are quantified using Prony analysis. In section V, concluding reflections, together with an outlook for future work are given.

II. Modified IEEE-39 Bus System

To perform this research, the IEEE-39 bus system has been used. A WPP plant has been added to bus 12 in the system as depicted in Fig. 1. The DIgSILENT FullyRatedConv WTG 6.0MW template is used to model a WPP of 175 aggregated wind turbines [17]. The WPP will operate at 5% of the rated power. The control parameters for the current controller and both PLLs are depicted in table I. At bus 6 a remote PMU signal is modelled as a PLL block. This block sends the voltage angle θ_{rem} to the control system of the WPP.

The control systems, which are described in the next paragraph, are tested during a disturbance of disconnecting transformer 11-12. This leads to a change of voltage angle and magnitude at bus 12 due to the changed impedance to the network. Before the system operates at a new stable operating point, the output power of the WPP will oscillate.

III. WPP Modified Control System

The control system of the WPP was modified in order to add WAD functionality. This is done by adding dynamic damping to the local PLL signal. This signal is used to transform the V_d and V_q signals to an abc frame. Using this implementation, most of the original control system will remain intact and make

TABLE I
Control Parameters of WPP Current Controller

Control Parameter	Value
$K_{p,d}$	0.2
$K_{p,q}$	0.2
$K_{i,d}$	40
$K_{i,q}$	40
$K_{PLL,p}$	100
$K_{PLL,i}$	3

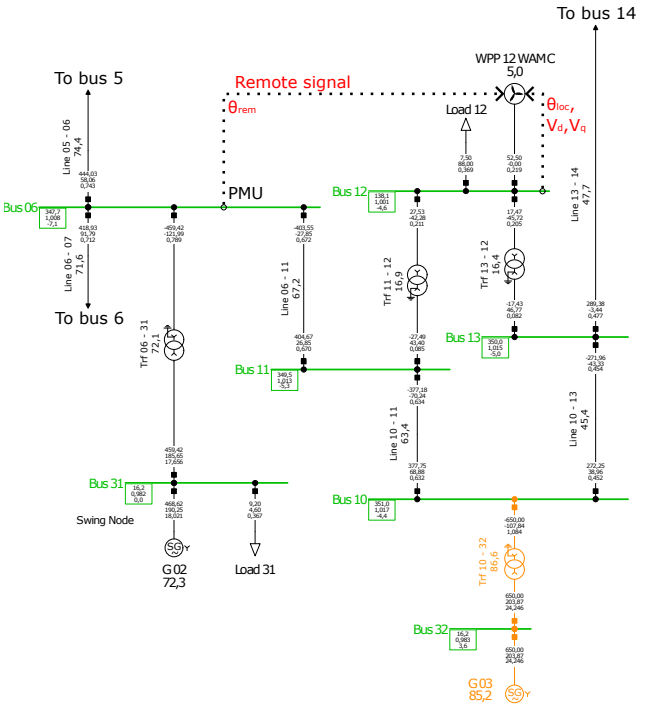

Fig. 1. Part of the modified IEEE-39 bus system around the connected WPP. Load flow results are shown, which show the equilibrium state before the disturbance. The measurements which are used as input for the control system are shown in red.

it easier to comprehend the workings of the damping. In the default situation, the signal voltage angle signal θ_{loc} of the local PLL is directly used for the inverse Park- and Clarke-transformation. As described in [9], PLL interaction can have a critical role in the amplification of a SSO.

The supplementary WAD is implemented to appropriately dampen local PLL signal oscillations. For this damping, an additional proportional control system is added. The gain factor $K\left(\omega_{rem}\right)$ is dynamically dependent on a remote signal. This relation is described in (1). In this case, only one remote signal is. However, more advanced schemes could be designed using more than one input signal.

$$K\left(\omega_{rem}\right) = K_{loc} + K_{rem}\omega_{rem} \tag{1}$$

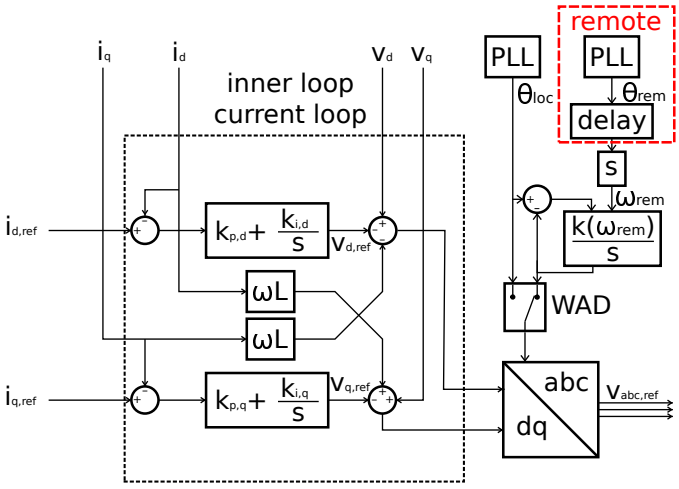

Fig. 2. Control system of the GSC of the WPP. The inner control loop is shown with the addition of a WAD system which can be turned on.

A remote PLL takes a measurement of the remote voltage angle at bus 6 (Fig. 1). This is communicated to the control system of the WPP. A time delay is modelled to accommodate for the communication and processing of this signal and is set to T_{delay} = 0.2 s. The remote signal θ_{rem} is differentiated to acquire the relative voltage angle speed ω_{rem}. This quantity is used to determine $K\left(\omega_{rem}\right)$. Two more gain parameters are used to tune the dynamic behaviour of $K\left(\omega_{rem}\right)$. K_{rem} is used to tune the dependence on the remote signal. Additionally, K_{loc} is introduced. This ensures that even if the remote voltage angle is stable, the voltage angle used for the Park- and Clarke- transformation will go to the local voltage angle and give a correct result. In this paper, values for the gain parameters were set to K_{loc} = 0.05 and K_{rem} = 1. More research can be performed to find the optimal tuning of these newly proposed gain parameters.

The intended behaviour is to dampen the amplification of a SSO. Because the oscillation will be less present further away from WPP, this implementation will dampen the PLL reaction to a SSO. If a different type of wider disturbance (e.g. frequency event), the WPP is still able to react quickly.

IV. Performance of WAD

To test the performance of the WAD, a disturbance event is introduced to the system. At t = 1 s, transformer 11-12 is disconnected and reconnected at t = 3 s. This event relevant because the change in impedance to the network will cause an voltage angle change. This will initiate a damped oscillation in the PLL of the control system. First, the modes in the case of the connected and disconnected transformer are compared when no WAD is used and when it is activated. These modes are obtained using eigenvalue analysis from a linearized dynamic model of the system. The system is also tested using a time domain simulation. Using Prony analysis, damping and frequency response to the disturbance are determined.

A. Eigenvalue analysis

Eigenvalue analysis is based on the linearization of the dynamic system in a stable operating point. A linear model is defined by (2) [18].

$$\frac{d\mathbf{x}}{dt} = \mathbf{A}\mathbf{x} \tag{2}$$

where $\mathbf{x}$ is a vector containing all state variables of the dynamic model. The complete system has 180 state variables without the WAD and 186 state variables when the WAD is implemented. $\mathbf{A}$ is a square matrix representing the dynamic behaviour of the state space model. Using 3) the (right) eigenvalues of this system are determined.

$$\mathbf{A}\boldsymbol{\phi}_j = \lambda_j \boldsymbol{\phi}_j \tag{3}$$

where $\boldsymbol{\phi}_j$ is the right eigenvector of mode j and λ_j is the corresponding complex eigenvalue. In each state space model, the number of modes is equal to the number of state variables. The real part of the eigenvalue σ_j represents the damping in the system of the mode, while the imaginary part ω_j represents the frequency of the mode. The damping ratio is calculated in (4) [18].

$$\zeta_j = \frac{-\sigma_j}{\sqrt{\sigma_j^2 + \omega_j^2}} \tag{4}$$

In Fig. 3, the results of the eigenvalue analysis of the system are shown. All eigenvalues are shown. The sub-synchronous modes of the WPP are very easy to distinguish from the lower frequency inter-area modes, which are known in the IEEE-39 bus system [19]. When both transformers are connected, the system is better damped due to the stronger connection of the WPP [11]. In both cases, the implementation of WAD has a significant positive effect on the damping and frequency of the sub-synchronous mode. The exact values are shown in table II. Because the damping (real part) increases and the frequency decreases, the damping ratio is positively influenced. The damping ratio is calculated using (4).

In addition to the eigenvalues, the participation factors of the sub-synchronous mode are compared. The participation factors are calculated using both the right and left eigenvector values. This results in dimensionless numbers representing the participation of a state variable in a mode. The participation factors are calculated in (5) and (6).

$$\boldsymbol{\psi}_k \mathbf{A} = \boldsymbol{\psi}_k \kappa_k \tag{5}$$

$$p_{j,k} = \boldsymbol{\phi}_{k,j} \boldsymbol{\psi}_{j,k} \tag{6}$$

TABLE II
Eigenvalues of sub-synchronous modes.

	1 transformer		2 transformers	
	λ_{SSO}	ζ_{SSO}	λ_{SSO}	ζ_{SSO}
No WAD	-7.3 + j96.1	0.07	-35.4 + j111.8	0.29
WAD	-20.2 + j68.5	0.28	-45.5 + j86.7	0.46

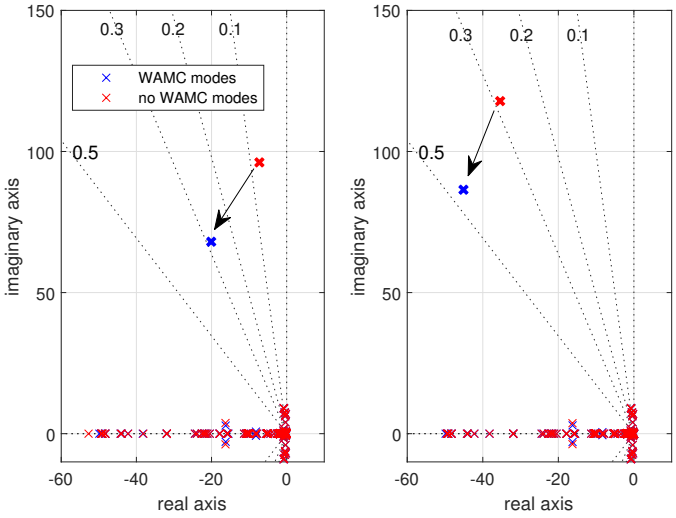

Fig. 3. Change in oscillation modes due to the implementation of a WAD at WPP. On the left, the situation for the disconnected transformer is shown. On the right, the situation with the transformer is shown. The damping ratio is indicated on the dotted diagonal lines.

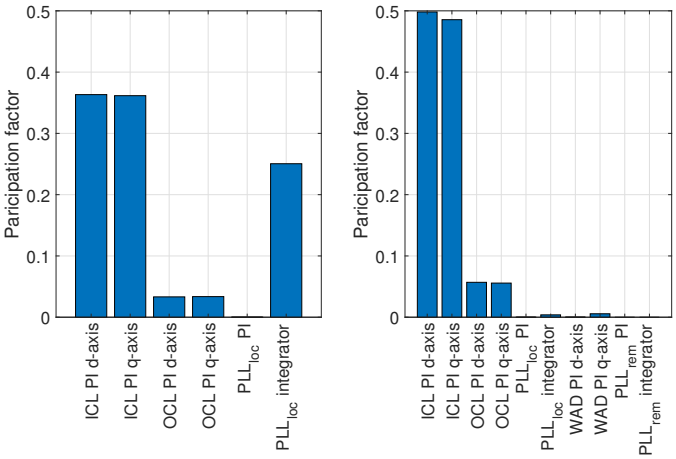

Fig. 4. Participation factors of state variables in the inner control loop (ICL), outer control loop (OCL), WAD and PLLs in sub-synchronous mode. Left shows the classic control system. Right shows the control system with the WAD implemented.

where $p_{j,k}$ represents the participation of state variable k in the j-th mode.

The participation factors related to the control system of the WPP are shown in Fig. 4. Participation factors not shown are 0.0045 or lower.

In the classic control system, the participation of the PLL is around 0.25, which is almost completely removed by the implementation of the WAD. It is expected the PLL is mostly influenced since the additional damping is focused on the voltage angle signal θ_{loc}. With the decrease in the participation of the PLL, the participation of the other state variables increases, which is expected as all participation factors of a mode sum to one.

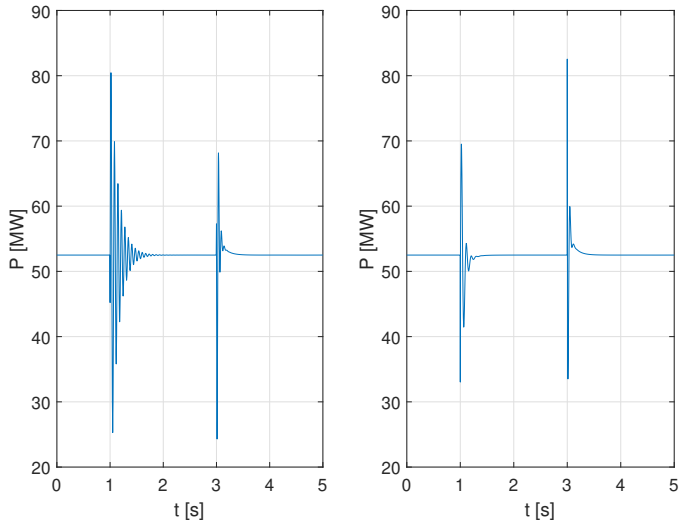

Fig. 5. Power output of WPP during disconnection and re-connection of transformer 11-12. On the left shows the results for no WAD implementation. On the right the results for the implementation of WAD are shown.

B. Time Domain Simulations

In Fig. 5, the power output of the WPP is shown. The results show clear power oscillations after the switch operations of transformer 11-12. At t = 1 s, the transformer is switched off. The oscillations correspond to the eigenvalue analysis with one transformer connected in the previous paragraph. When the system is stabilized at t = 3 s, the transformer is reconnected, which corresponds to the eigenvalue analysis of two connected transformers.

In Fig. 5, the ring downtime without WAD is much longer compared to when the WAD is implemented. To quantify these results, Prony analysis after each switching event. A damped sinusoidal function is fitted on the ring down function, which yields the damping and frequency after the disturbance as shown in (7) [20].

$$\Delta P(t) = a \sin(\omega_{SSO} t + \phi) e^{\sigma_{SSO} t} \tag{7}$$

where a and ϕ are necessary parameters to fit the function but are dependent on the placement of the Prony window. ω_{SSO} and σ_{SSO} will yield the frequency and damping of the oscillations.

In Fig. 6, the Prony windows are shown. In these zoomed results, it is visible that the first swing of the oscillations is also positively influenced by the WAD. Using the depicted Prony windows and function (7), the results shown in Table III are obtained. As the time response is a superposition of all modes with amplitudes depending on the disturbance, care should be taken in the placement of the Prony window. As there exist modes with a lower frequency and less damping, the Prony windows are placed as close to the start of the oscillation as possible. Less damped modes will have a relatively larger amplitude longer after the disturbance has taken place. Because the disturbance is focused on the WPP, other modes are

TABLE III
RESULTS OF PRONY ANALYSIS ON POWER OSCILLATIONS.

	1 transformer			2 transformers		
	σ_{SSO} [s^{-1}]	ω_{SSO} [rad/s]	ζ_{SSO}	σ_{SSO} [s^{-1}]	ω_{SSO} [rad/s]	ζ_{SSO}
No WAD	-5.7	94.8	0.06	-38.3	101.9	0.35
WAD	-13.1	62.6	0.20	-44.9	94.0	0.43

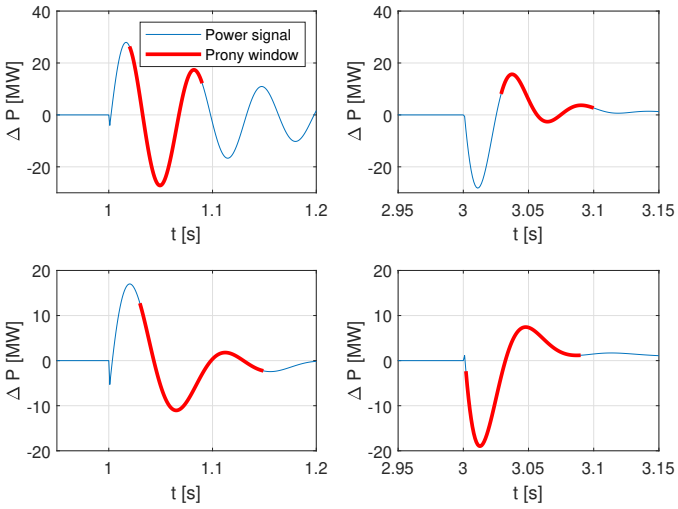

Fig. 6. Prony analysis of power output oscillations ΔP after switching of transformer 11-12. On top, oscillations without WAD are shown, and below the oscillation with the implementation of the WAD are shown.

expected to have little influence directly after the disturbance. The Prony analysis shows similar improvements by the WAD as the eigenvalue analysis. It is also conformed the system is generally better damped with both transformers connected.

V. CONCLUSIONS

This paper proposes a WAD system to dampen the SSO induced by the control system of PEIG. The proposed WAD uses a remote voltage angle signal which can be measured by a PMU. The PMU signal is to be communicated quickly to the control system of the GSC of the WPP. This signal is only used for supplementary damping of the local voltage angle. This results in a simple addition to the existing control system. This approach makes implementation easier, as it is only an extra layer to the control system which can switch on or off.

The performance is tested within the IEEE-39 bus using both eigenvalue analysis and the time response of the system after a disturbance. The eigenvalue analysis shows a significant improvement when the WAD is implemented. This is confirmed by the Prony analysis on the time response of the power output oscillations after a disturbance. The participation factors in the eigenvalue analysis show the almost complete removal of the PLL in sub-synchronous mode due to the implementation of the WAD.

Future work could explore the WPP response to different disturbances, such as frequency events. Also, the optimal placement and tuning of the PMU has the potential for further improvements. Furthermore, the option of more than one remote PMU could be considered. This would lead to a more complex control system, but if designed properly, more resilient to disturbances.

REFERENCES

[1] European Commission, "The European Green Deal", Brussels, Belgium, December 2019

[2] Qin, B, et al., "Quantitative short-term voltage stability analysis of power systems integrated with DFIG-based wind farms", IET Generation, Transmission & Distribution, vol. 14.19, pp. 4264-4272, 2020

[3] Adams, J., Carter, C. and Huang, S. H., "ERCOT Experience with Sub-Synchronous Control Interaction and Proposed Remediation", Proceedings of the IEEE Power Engineering Society Transmission and Distribution Conference, 2012.

[4] National Grid ESO, "Technical Report on the Events of 9 August 2019", technical report, 2019.

[5] Sewdien, V., Wang, X., Torres, J. R. and Van Der Meijden, M., "Critical Review of Mitigation Solutions for SSO in Modern Transmission Grids", July 2020.

[6] Yunhong, L., Hui, L., Xiaowei, C., Jing, H. and Ul I, Y., "Impact of PMSG on SSR of DFIGs Connected to Series-Compensated Lines Based on the Impedance Characteristics", The Journal of Engineering, 2017.

[7] Narendra, K. et al., "New Microprocessor Based Relay to Monitor and Protect Power Systems against Sub-Harmonics", 2011 IEEE Electrical Power and Energy Conference, EPEC 2011, pp. 438–443, 2011.

[8] NERC, "Lesson Learned - Sub-Synchronous Interaction between Series-Compensated Transmission Lines and Generation", tech. rep., Atlanta, USA, July 2011.

[9] Xu, Y. and Cao, Y., "Sub-Synchronous Oscillation in PMSGs Based Wind Farms Caused by Amplification Effect of GSC Controller and PLL to Harmonics", IET Renewable Power Generation, vol. 12, pp. 844–850, 2018.

[10] Xu, Y., Zhao, S., Cao, Y. and Sun, K., "Understanding Subsynchronous Oscillations in DFIG-Based Wind Farms Without Series Compensation", IEEE Access, vol. 7, pp. 107201–107210, 2019.

[11] Liu, H. et al., "Subsynchronous Interaction Between Direct-Drive PMSG Based Wind Farms and Weak AC Networks", IEEE Transactions on Power Systems, vol. 32, pp. 4708–4720, November 2017.

[12] Yan, G., Wan, Q., Jia, Q. and Liu, J., "Analysis of SSO Characteristics of D-PMSGs Based Wind Farm under Weak AC System", 2nd IEEE Conference on Energy Internet and Energy System Integration, EI2 2018 - Proceedings, December 2018.

[13] Adib, A., Mirafzal, B., Wang, X. and Blaabjerg, R., "On Stability of Voltage Source Inverters in Weak Grids", IEEE Access, vol. 6, pp. 4427–4439, December 2017.

[14] Du, W., Wang, X. and Wang, H., "Sub-Synchronous Interactions Caused by the PLL in the Grid-Connected PMSG for the Wind Power Generation", International Journal of Electrical Power and Energy Systems vol. 98, pp. 331–341, June 2018.

[15] Li, Y., Fan, L. and Miao, Z., "Wind in Weak Grids: Low-Frequency Oscillations, Subsynchronous Oscillations, and Torsional Interactions", IEEE Transactions on Power Systems, vol. 35, pp. 109–118, January 2020.

[16] Shair, J., Xie, X. and Yan, G., "Mitigating subsynchronous control interaction in wind power systems: Existing techniques and open challenges", Renewable and Sustainable Energy Reviews, vol. 108, pp. 330-346, 2019

[17] DIgSILENT GmbH, "Technical Reference DIgSILENT Fully Rated Converter Wind Turbine Templates", DIgSILENT PowerFactory GmbH, tech. rep., Gomaringen, Germany, 2022.

[18] Kundur, P.S., and Malik, O.P., "Power System Stability and Control", McGraw-Hill Education, 2022.

[19] DIgSILENT GmbH, "39 Bus New England System", DIgSILENT PowerFactory GmbH, tech. rep., Gomaringen, Germany, 2020.

[20] Hauer, J.F.,"Application of Prony Analysis to the Determination of Modal Content and Equivalent Models for Measured Power System Response", IEEE Transaction on Power Systems, vol. 6.3, pp. 1062-1068, 1991